

## Functionalization of surgical meshes with antibacterial hybrid Ag@*crowns* nanoparticles

U. A. Hasanova<sup>a</sup>, A. R. Aliyev<sup>a,e,\*</sup>, I. R. Hasanova<sup>a,e</sup>, E. M. Gasimov<sup>b</sup>,  
S. F. Hajiyeva<sup>a,e</sup>, A. A. Israyilova<sup>c,e,f</sup>, Kh. G. Ganbarov<sup>d</sup>, Z. O. Gakhramanova<sup>e</sup>,  
P. F. Huseynova<sup>g</sup>, N. R. Amrahov<sup>c,e,f</sup>

<sup>a</sup>*Baku State University, Chemical Department, Z.Khalilov 23, AZ 1148 Baku, Azerbaijan*

<sup>b</sup>*Azerbaijan Medical University, Surgical Department Bakikhanov str. 23, AZ 1022, Baku, Azerbaijan*

<sup>c</sup>*Department of Molecular biology and Biotechnology, Baku State University, Z.Khalilov 23, AZ 1148 Baku, Azerbaijan*

<sup>d</sup>*Laboratory of Microbiology and Virology, Baku State University, Z.Khalilov 23, AZ1148, Baku Azerbaijan*

<sup>e</sup>*Azerbaijan State Oil and Industry University, Azadliq Ave 16/21, AZ1010, Baku, Azerbaijan*

<sup>f</sup>*Azerbaijan Research Institute of Crop Husbandry, Ministry of Agriculture, Pirshagi settlement, AZ1098, Baku, Azerbaijan*

<sup>g</sup>*Ganja State University, Chemical Department, Shah Ismayil Khetayi Ave, Ganja, Azerbaijan*

We report here on functionalization of surgical meshes (PVDF) with novel hybrid material, consisting of Ag@*crowns* nanoparticles, embedded on CaCO<sub>3</sub>/PEG nanosheets. Nanosheets of PEG 4000 with average thickness of 25 nm enclosing CaCO<sub>3</sub> nanoparticles with average sizes of 150 nm were applied for sustained release of Ag@*crowns* nanoparticles that in turn serve as antibacterial agent. The characterization of obtained hybrid nanostructures was carried out by microscopic and spectroscopic methods. Microbiological tests confirmed the effectiveness of hybrid material, consisting of Ag@*crowns* nanoparticles, embedded in CaCO<sub>3</sub>/PEG nanostructure, as an antibacterial coating for surgical meshes. This coating was applied to insure antibacterial properties of meshes against microorganism colonization, in order to significantly improve their action in typical applications.

(Received September 10, 2021; Accepted January 7, 2022)

**Keywords:** Silver nanoparticles, Calcium carbonate, CaCO<sub>3</sub>/PEG nanostructures, Controlled release, Surgical meshes

### 1. Introduction

The functionalization of surgical meshes with various antibacterial agents can significantly improve their characteristics and minimize the number of postsurgical complications. There are numerous reports of immobilization of surface of the surgical meshes with antibiotics and antibiotics containing composites [1-3]. However, the functionalization of medical devices with antibiotics often does not satisfy the expectations of prolonged action, due to their fast removal in the biological liquids. At the same time, considering the growing antimicrobial resistance towards existing antibiotics, we propose the functionalizing of the surface of PVDF surgical meshes with new hybrid material, consisting of Ag@*crowns* nanoparticles embedded in PEG 4000 nanosheets incorporating CaCO<sub>3</sub> nanoparticles. The applications of Ag ions and nanoparticles as a very effective antimicrobial agent, even against resistant strains of microorganisms, are proved by

---

\* Corresponding authors: alibalaaliyev@bsu.edu.az  
<https://doi.org/10.15251/DJNB.2022.171.11>

numerous studies [4,5] and some of them are commercialized [6-9]. In our previous studies we reported of synthesis and antimicrobial activity of Ag@Crown nanocomposite. In this study it has been found that chelating of Ag with diazacrown ether allows to reduce the MIC of silver nanoparticles hundreds of times that may lead to diminishing of their toxic and adverse effects [10].

It also should be noted that sustainable controlled release of Ag nanoparticles is necessary, in order to avoid the cumulation of high concentration of silver nanoparticles in the organism and, as consequence, the possible occurrence of toxicity [11]. For this purpose different methods for controlled release of Ag nanoparticles were developed, among them immobilization of Ag nanoparticles in the polymer matrix [12], glass [13], silica [14], natural fibers [15,16], hydroxyapatite [17], on the metal surface [18] and application of calcium carbonate nanoparticles [19]. The stability, slow biodegradability and non-toxicity make  $\text{CaCO}_3$  nanoparticles promising candidate for sustained-release of drugs [20]. Beside this, at the present time there is no data of the application of hybrid material representing PEG 4000 nanosheets enclosing calcium carbonate nanoparticles as sustained release drug carrier.

Thus, the purpose of given study was to functionalize surgical meshes with antimicrobial coating, based on nanocomposite of silver nanoparticles, chelated by diazacrown-ether and immobilized on the surface of  $\text{CaCO}_3$ /PEG nanomaterial.

## 2. Materials and methods

Silver nitrate, calcium chloride ( $\text{CaCl}_2$ ), ammonium hydroxide ( $\text{NH}_4\text{OH}$ ), hydrochloric acid (98%), nitric acid (65%), polyethylene glycol 4000 (PEG 4000), starch, sodium chloride ( $\text{NaCl}$ ), ethanol were purchased from Sigma-Aldrich (Darmstadt, Germany), Muller Hinton broth was purchased from Biolife (Milan, Italy) and were used without purification. Deionized water was used in all experiments. Buffers were prepared by mixing appropriate amounts of 0.1M citric acid and 0.2  $\text{Na}_2\text{HPO}_4$ . Sterile PVDF meshes were obtained from Lintex LLC (Russia) and were made correspondingly from polypropylene and polyvinylidene fluoride monofilaments with a diameter of 0.12 mm and a pore sizes  $>1$  mm.

**Synthesis of Ag@Crown.** Synthesis of Ag nanoparticles was carried out by “green” synthesis method, using starch [21]. In the first step 25 mg of starch, dissolved in 50 ml of deionized water was mixed with 30 mg of  $\text{AgNO}_3$  dissolved in 50 ml of deionized water. After that, the 25% ammonia was added until  $\text{pH} \approx 11$ . The received solution was agitated in an ultrasonic bath during one hour with cooling. Further, obtained brown colloid was centrifuged at 4,000 rpm for 5 min and precipitated Ag nanoparticles were repeatedly washed with deionized water to remove the water-soluble ammonium nitrate. The washing process was repeated three times and the product was dried under a stream of nitrogen at ambient. In the second step, synthesis of Ag@Crown nanoparticles was performed by dispersion of Ag nanoparticles powder dispersed in ethanol and mixing it with the ethanol solution of diazacrown ether. The obtained mixture was agitated in an ultrasonic bath for 15 minutes. Then obtained Ag@Crown nanoparticles were dried under a stream of nitrogen at ambient.

The morphology analysis was carried out by employing transmission electron microscopy (TEM) JEM-1400 (Japan) at 80-120 kV. For this, small amount of Ag@Crown powder was taken to prepare ethanol dispersion. The drop of this dispersion was placed on carbon coated copper grid for TEM studies.

### 2.1. Synthesis of graphene-like $\text{CaCO}_3$ nanolayers

0.6 g of calcium chloride and 0.015 g of PEG 4000 were dissolved in 50 ml of deionised water, and the solution was heated to  $60^\circ\text{C}$ . Afterwards, while keeping the temperature of  $60^\circ\text{C}$ , the stoichiometric quantity of  $\text{NH}_4\text{OH}$  aqueous solution was added dropwise, whilst gaseous carbon dioxide was bubbled through the solution in flask under intense stirring. Since addition of base was carried out for 2 hours, refluxing was used for this system throughout synthesis. After addition of base, white precipitate was obtained, and the obtained mixture was kept under the same conditions of intense stirring and temperature of  $60^\circ\text{C}$  for the next 1.5 hours. Subsequently, the

mixture was left cooling to room temperature, followed by several repeated vacuum filtrations of the mixture. The precipitate, accumulated on glass filter, was washed with deionized water and ethanol. The small amount of obtained powder was taken to prepare ethanol dispersion. The drop of this dispersion was placed on carbon coated copper grid for TEM studies by employing transmission electron microscope (TEM) JEM-1400 (Japan) at 80-120 kV.

## **2.2. Preparation of Ag@Crown/CaCO<sub>3</sub> nanostructures and mesh surface modification with obtained hybrid nanostructures.**

1.2 mg of Ag@Crown was dispersed in 50 ml of deionised water and agitated in an ultrasonic bath for 15 minutes. Then, aqueous solution of CaCO<sub>3</sub>/PEG nanosheets was poured into the solution of Ag@Crown. The solution was stirred for 12 h at room temperature using a magnetic stirrer at 150 rpm. The overall concentrations of Ag and diazacrown ether in the prepared solution of Ag@Crown/CaCO<sub>3</sub>/PEG nanosheets were 0.25 µg/mL and 0.125 µg/mL correspondingly.

For mesh surface modification the PVDF samples of meshes with 1x1 cm size were immersed in the prepared solution of Ag@Crown/CaCO<sub>3</sub>/PEG hybrid nanostructures. Further, the meshes were dried under a stream of nitrogen.

## **2.3. Characterization of hybrid nanostructures and surface modified meshes**

The morphology analysis was carried out by transmission electron microscopy (TEM) on JEM-1400 (Japan) at 80-120 kV. The morphology analysis of the mesh coated with Ag@Crown/CaCO<sub>3</sub>/PEG nanostructures was carried out by employing Field Emission Scanning Electron Microscope JEOL JSM-7600F at an accelerating voltage of 15.0 kV, SEI regime.

## **2.4. Accelerated release of Ag nanoparticles from surface modified meshes**

The samples of surface modified meshes were immersed in 8 ml of the appropriate buffer solutions with pH values equal to 6.5-6.8. The pH values were chosen, according to the fact that infected peritoneal fluid has pH < 7.1 [22]. They were vigorously stirred for a given period of time and then centrifuged. Supernatants were collected for ICP analyses and the next portions of fresh buffer solutions were added each time. The procedure was continued for 14 days.

## **3. Antibacterial test**

The antibacterial activity of meshes, containing Ag@Crown, Ag@Crown/CaCO<sub>3</sub>/PEG and CaCO<sub>3</sub>/PEG, against *S.aureus* BDU23 and *P.aeruginosa* BDU49 was studied by measuring zone of inhibition [23]. Bacterial strains were taken from culture collections of the Department of Microbiology of Baku State University (Azerbaijan). The optical density of the overnight bacterial cultures in Muller Hinton broth (MHB) was adjusted to 0.5 McFarland ( $1.5 \times 10^8$  cfu/mL) by diluting in saline solution (0.8% NaCl). Then 100 µl of bacterial culture suspension was spread on sterile Muller Hinton Agar (MHA) plates, and the plates were kept about 10 min. The meshes, modified with Ag@Crown, Ag@Crown/CaCO<sub>3</sub>/PEG and CaCO<sub>3</sub>/PEG, were gently placed at the centre of the MHA in different Petri dishes. Plates were incubated at 37°C for 24 h. After incubation the antibacterial properties of functionalized meshes were evaluated, according to the diameter of the inhibition zone (mm).

## **4. Results and discussions**

Modern hernia repair techniques (hernioplasty), using synthetic polymer (polyvinylidene fluoride PVDF) endoprostheses, can significantly improve the results of surgical treatment of abdominal wall hernias [24]. As with all surgical procedures, surgical wounds that require the use of synthetic non-absorbable implants, such as surgical meshes, may be susceptible to infection [25,26]. Moreover, even if meshes are provided for use in a sterile state, they can nevertheless serve as a basis for the infection occurrence by providing a substrate for attachment of bacteria and formation of a biofilm [27]. Such biofilms can be extremely resistant to the treatment with

conventional and affordable antibiotics, and also can be life-threatening. Thus, for non-absorbable surgical implants, such as surgical meshes for treating a hernia, a long-term or even permanent antimicrobial surface is desirable. We modify the meshes surface by immersing of the samples of PVDF meshes in the colloid solution of prepared hybrid Ag@Crown/CaCO<sub>3</sub>/PEG nanostructures. A significant feature for modifying a meshes with antimicrobial properties is the treatment of PVDF meshes with colloid solutions, containing supramolecular complexes of ultra-disperse silver nanoparticles with diazacrown ethers, embedded into CaCO<sub>3</sub>/PEG nanosheets, which may provide a prolonged antimicrobial effect.

Considering the growth of microbial resistance towards antibiotics, we used the Ag@Crown nanostructures as the main component of antibacterial coating for PVDF surgical meshes for hernia repair. For this purpose, we carried out the chelation of silver nanoparticles with diazacrown ethers by means of noncovalent interactions. Ag@Crown nanoparticles were prepared by reduction of silver nitrate with applying the ultrasound waves and following chelating of obtained Ag nanoparticles with diazacrown ethers. Previously it has been shown that chelation of Ag nanoparticles with diazacrown ethers significantly diminished minimal inhibitory concentrations of silver nanoparticles [28]. The obtained samples of Ag@Crown were examined by TEM analysis (Fig.1)

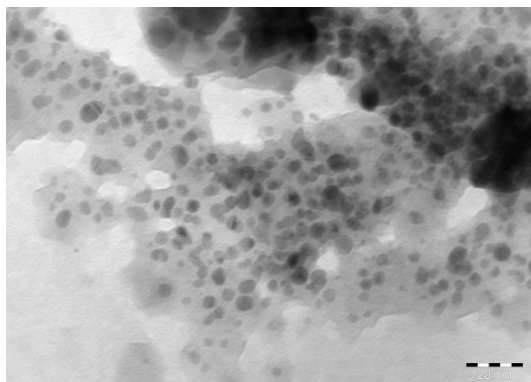


*Fig. 1. TEM image of Ag@Crown nanoparticles.*

As it seen from the Figure 1(a) the Ag@Crown nanoparticles have uniformed spherical shape and their sizes differ in the range 5-12 nm. Such narrow size distribution can be due to the coating of the surface of formed silver nanoparticles with starch molecules. The starch that have been used as reducer, in this case, also serve as stabilizer to prevent the growth of sizes of formed nanoparticles. The coupling of Ag nanoparticles with diazacrown ether is reasonable, since crown ethers behave like ionophores that can integrate into the membrane of a bacterial cell, violating its membrane potential. At the same time crown ether molecules, adsorbed on the surface of Ag nanoparticles, also prevent agglomeration process.

Calcium carbonate in its micro and nano sizes modified with PEG has been shown to be efficient drug delivery agent (37,40,53), however, there is no information of application of CaCO<sub>3</sub>/PEG nanosheets hybrid structure as carrier. It can be assumed that due to high surface area of calcium carbonate nanoparticles dispersed within PEG nanosheets and partially covered by them, this nanostructure possesses high activity, which leads to better adsorption of Ag@Crown nanoparticles. For this reason, we suggested to use this nanomaterial for sustained release drug system. In present study we consider following possible mechanism for the formation of CaCO<sub>3</sub>/PEG hybrid structure under reported conditions. At the first stage, Ca<sup>2+</sup> binds to PEG to form alkoxide. Afterwards, when CO<sub>2</sub> is dissolved in water by its slow bubbling through abovementioned solution, carbonate anions form and bind to Ca<sup>2+</sup> to completely replace PEG. However, PEG being in coordination sphere of Ca<sup>2+</sup> coordinates to the cations with O atoms. Upon cooling, filtration and drying PEG molecules recrystallise to form nanosheets while keeping strong affinity with CaCO<sub>3</sub> nanoparticles. The TEM images of obtained hybrid structure is shown on Figure 2.

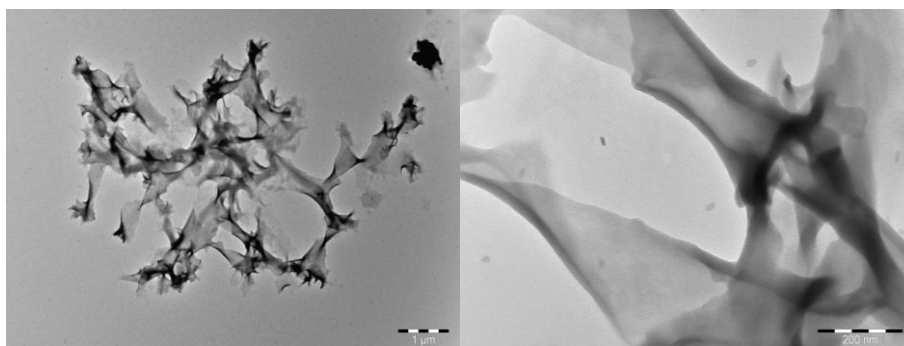


*Fig. 2. TEM images of CaCO<sub>3</sub>/PEG nanosheets hybrid nanomaterial.*

Figure 2 reveals PEG 4000 nanosheets with high surface area containing CaCO<sub>3</sub> nanoparticles. Basing on measurements from TEM images the average sizes of CaCO<sub>3</sub> nanoparticles were calculated to be 150 nm while average thickness of PEG 4000 nanosheets was calculated to be 25 nm. It should be noted that basing on measurement of mass of product we can state that portion of PEG in CaCO<sub>3</sub>/PEG hybrid was less than 1.1 % from the whole mass of hybrid nanostructure.

In order to prepare the hybrid Ag@*crown*/CaCO<sub>3</sub>/PEG nanostructures, the obtained Ag@*crown* nanoparticles were embedded to CaCO<sub>3</sub>/PEG nanostructure. The resulting colloidal solution of prepared hybrid Ag@*crown*/CaCO<sub>3</sub>/PEG nanostructures then was analysed by TEM.

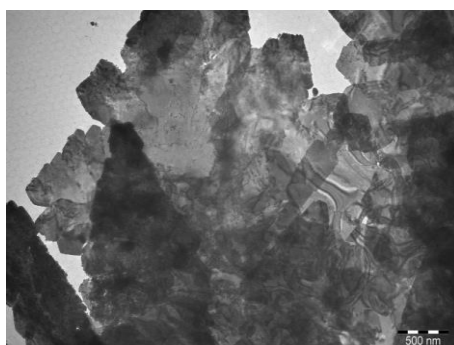


*Fig. 3. TEM image of Ag@*crown*/CaCO<sub>3</sub>/PEG nanoparticles.*

As it can be seen from the Figure 3 the hybrid Ag@*crown*/CaCO<sub>3</sub>/PEG nanostructures represent Ag@*crown* distributed in PEG 4000 nanosheets with incorporated CaCO<sub>3</sub> nanoparticles

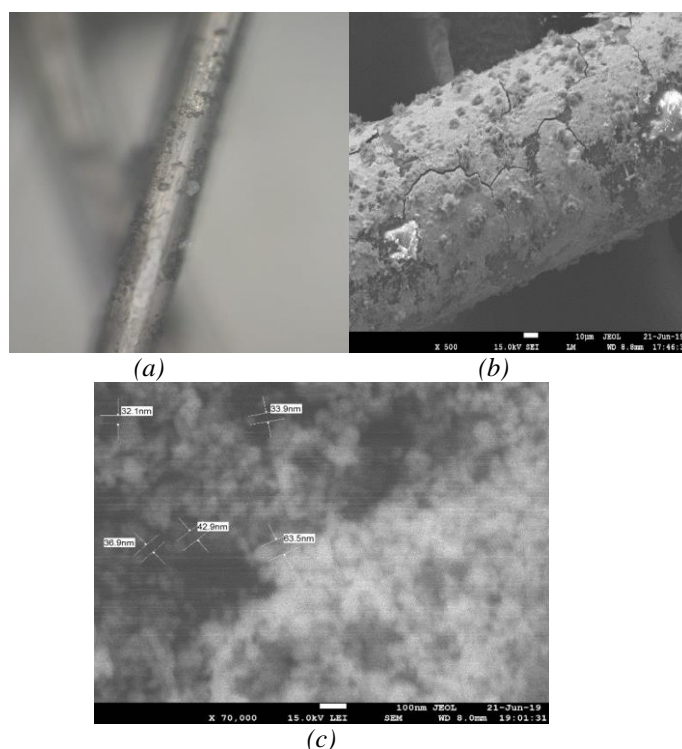


Fig. 4. a) Optical microscopy of PVDF meshes modified with hybridAg@crown/CaCO<sub>3</sub>/PEG nanostructures; b, c) SEM images of PVDF meshes modified with hybridAg@crown/CaCO<sub>3</sub>/PEG nanostructures

Ag@crown/CaCO<sub>3</sub>/PEG were adsorbed to PVDF meshes successfully (Figure 4). The 2D structure of PEG provides the strong adhesion, lowering penetration of antimicrobial agent into the structure of mesh monofilaments, and prepares their surface for the subsequent formation of a silver nanostructured coating with a particle size of 10 to 20 nm. Also, in favor of the firm attachment of hybrid nanostructure to the surface of mesh speaks that high vacuum condition, applied during SEM analyses, did not affect them and we could clearly observe their presence and structure. In Figure 4 are given images modified with hybrid Ag@crown/CaCO<sub>3</sub>/PEG nanostructures PVDF meshes, made by optical and scanning electron microscopy techniques.

Table 1. The antibacterial test results against *S. aureus* and *P. aeruginosa*.

Bacterial strains	Zone of inhibition of tested compounds			
	Mesh with Ag@crown	Mesh with Ag@crown/CaCO <sub>3</sub> /PEG nanosheets	Mesh with CaCO <sub>3</sub> /PEG nanosheets	PVDF meshes
<i>Staphylococcus aureus</i> BDU23	29 ± 0.57	20 ± 0.48	-	-
<i>Pseudomonas aeruginosa</i> BDU49	28 ± 2.33	18 ± 0.48	-	-

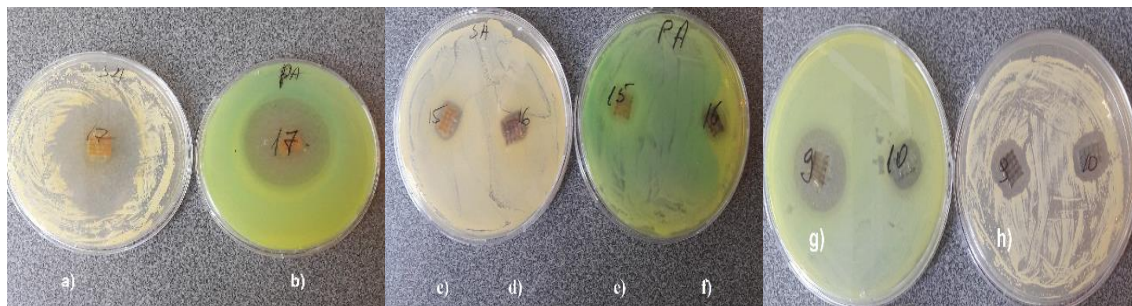


Fig. 5. Photographs of antibacterial test: a) Mesh with Ag@Crown on *S. aureus* BDU23; b) Mesh with Ag@Crown on *P. aeruginosa* BDU49; c) Mesh with CaCO<sub>3</sub>/PEG nanosheets on *S. aureus* BDU23; d) PVDF mesh on *S. aureus* BDU23; e) Mesh with CaCO<sub>3</sub>/PEG nanosheets on *P. aeruginosa* BDU49; f) PVDF mesh on *P. aeruginosa* BDU49; g) Mesh with Ag@Crown/CaCO<sub>3</sub>/PEG on *P. aeruginosa* BDU49; h) Mesh with Ag@Crown/CaCO<sub>3</sub>/PEG on *S. aureus* BDU23

As it can be seen from the Table 1 the surgical mesh, functionalized with Ag@Crown demonstrated the highest antibacterial activity against selected bacterial strains. The diameter of inhibition zone on *S. aureus* BDU23 was equal to  $29 \pm 0.57$  mm, on *P. aeruginosa* BDU49 -  $28 \pm 2.33$  mm. There was no significant difference between Gram-positive and Gram-negative bacteria. Functionalization of mesh with Ag@Crown/CaCO<sub>3</sub>/PEG hybrid nanostructure leads to the reduction of the inhibition zone both on *P. aeruginosa* BDU49 and *S. aureus* BDU23 approximately by 10 mm ( $20 \pm 0.48$  mm on *S. aureus* BDU23;  $18 \pm 0.48$  mm on *P. aeruginosa* BDU49). Any antibacterial effect was not detected against *S. aureus* BDU23 and *P. aeruginosa* BDU49 when tested with the non-functionalized mesh and mesh with the CaCO<sub>3</sub>/PEG nanostructure. (Figure 5). From the results of antibacterial test, it can be inferred that that Ag@Crown nanoparticles retain their antimicrobial activity in the composition of Ag@Crown/CaCO<sub>3</sub> hybrid nanostructure. The reduction in value of inhibition zone can be connected with sustained release of Ag@Crown, provided by the effect of CaCO<sub>3</sub>/PEG carrier. Application of Ag@Crown in a form of Ag@Crown/CaCO<sub>3</sub>/PEG hybrid nanostructure may limit the toxicity of silver nanoparticles to human cells and make possible their long-term influence.

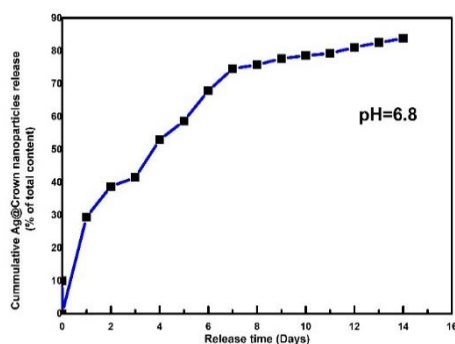


Fig. 6. Sustained release of Ag@Crown nanoparticles into buffer solution.

Sustained release of silver nanoparticles from the meshes' surface into the buffer solutions was studied by ICP-OES and AAS. The results of both methods show good correlation with each other. As it can be inferred from the Figure 6 Ag@Crown nanoparticles can be slowly released over long period of time from the surface of PVDF meshes. Rapid release of Ag@Crown nanoparticles in first 72 hours in the buffer solutions and equal to ca. 42% can be attributed to the presence of the most loosely attached fraction of nanoparticles. The efficient burst release of antimicrobial agent is valuable, because it will prevent the attachment of bacteria and biofilm formation on the surface of implanted meshes [29]. Further release of Ag@Crown nanoparticles is

much slower, reaching sustained release on the seventh day of the experiment, and that can be explained by deeper embedment and more firmly attachment of nanoparticles to the matrix. Also, slow disintegration and dissolution of CaCO<sub>3</sub> nanoparticles can take place.

## 5. Conclusion

The functionalization of and PVDF surgical meshes with hybrid Ag@Crown/CaCO<sub>3</sub>/PEG nanostructures gave them antibacterial property against *Pseudomonas aeruginosa* BDU49 and *Staphylococcus aureus* BDU23 that can last over 14 days, due to sustained release of an active compound. The efficiency of CaCO<sub>3</sub>/PEG nanostructures as a sustained drug release agent has been tested, and it was revealed that they are a good candidate for the creation of an antimicrobial drug sustained release system with the application as a coating for surgical meshes. Sustained release of Ag@Crown nanoparticles from Ag@Crown/CaCO<sub>3</sub>/PEG hybrid nanostructure was reached on seventh day of the sustained release test. Considering that surgical meshes have to be able to prevent the occurrence of infection at the site of implantation, their functionalization with Ag@Crown/CaCO<sub>3</sub>/PEG nanostructure is an efficient approach for giving them desirable properties.

## References

- [1] E. M. Benetti, X. Sui, S. Zapotoczny, G. J. Vancso, *Advanced Functional Materials* 20(6), 939 (2010); <https://doi.org/10.1002/adfm.200902114>
- [2] C. D. Klink, K. Junge, M. Binnebosel, H. P. Alizai, J. Otto, U. P. Neumann, U. Klinge
- [3] W. Cai, H. Hofmeister, T. Rainer, W. Chen, *Journal of Nanoparticle Research* 3(5), 441 (2001); <https://doi.org/10.1023/A:1012537817570>
- [4] B. Calderón-Jiménez, M. E. Johnson, A. R. Montoro Bustos, K. E. Murphy, M. R. Winchester, J. R. Vega Baudrit, *Frontiers in Chemistry* 5, 6 (2017); <https://doi.org/10.3389/fchem.2017.00006>
- [5] H. Cao, X. Liu, *Wiley Interdiscip Rev* 2(6), 670 (2010); <https://doi.org/10.1002/wnan.113>
- [6] L. Chen, L. Zheng, Y. Lv, H. Liu, G. Wang, N. Ren, D. Liu, J. Wang, R. I. Boughton, *Comparison of Long-Term Biocompatibility of PVDF and PP Meshes* (2010).
- [7] Z. Dong, L. Feng, W. Zhu, X. Sun, M. Gao, H. Zhao et al., *Biomaterials* 110, 60 (2016); <https://doi.org/10.1016/j.biomaterials.2016.09.025>
- [8] N. Durán, M. Durán, M. B. De Jesus, A. B. Seabra, W. J. Fávaro, G. Nakazato, *Nanomedicine: Nanotechnology, Biology and Medicine* 12(3), 789 (2016); <https://doi.org/10.1016/j.nano.2015.11.016>
- [9] M. Gimeno, P. Pinczowski, M. Pérez, A. Giorello, M. Á. Martínez, J. Santamaría, M. Arruebo, L. Luján, *European Journal of Pharmaceutics and Biopharmaceutics* 96, 264 (2015); <https://doi.org/10.1016/j.ejpb.2015.08.007>
- [10] S. Hajiyeva, U. Hasanova, Z. Gakhramanova, A. Israyilova, K. Ganbarov, E. Gasimov, F. Rzayev, G. Eyvazova, A. Huseynzada, G. Aliyeva, I. Hasanova, *Turkish Journal of Chemistry* 43(6), 1711 (2019); <https://doi.org/10.3906/kim-1907-10>
- [11] Ketan Vagholkar, Amish Pawanarkar, Suvarna Vagholkar, Madhavan Iyengar, Shamsershah Pathan, *International Surgery Journal* 3(2), 950 (2016); <https://doi.org/10.18203/2349-2902.isj20160701>
- [12] H. R. Kim, M. J. Kim, S. Y. Lee, S. M. Oh, K. H. Chung, *Mutation Research* 726(2), 129 (2011); <https://doi.org/10.1016/j.mrgentox.2011.08.008>
- [13] C. Labay, J. M. Canal, M. Modic, U. Cvelbar, M. Quiles, M. Armengol, M. A. Arbos, F. J. Gil, C. Canal, C., *Biomaterials* 71, 132 (2015); <https://doi.org/10.1016/j.biomaterials.2015.08.023>
- [14] G. E. Leber, J. L. Garb, A. I. Alexander et al., *The Archives of Surgery* 133(4), 378 (1998); <https://doi.org/10.1001/archsurg.133.4.378>

- [15] Y. Lv, H. Liu, Z. Wang, L. Hao, Y. Liu, Y. Wang, G. Du, D. Liu, J. Zhan, J. Wang, *Polymers for Advanced Technologies* 19(11), 1455 (2008).
- [16] Y. Lv, H. Liu, Z. Wang, S. Liu, L. Hao, Y. Sang, D. Liu, J. Wang, R. I. Boughton, *Journal of Membrane Science* 331(1-2), 50 (2009); <https://doi.org/10.1016/j.memsci.2009.01.007>
- [17] Maciej Długosz, Maria Bulwan, Gabriela Kania, Maria Nowakowska, Szczepan Zapotoczny, *Journal of Nanoparticle Research*, (2012).
- [18] A. Mackevica, M. E. Olsson, S. F. Hansen, *Journal of hazardous materials* 322, 270 (2017); <https://doi.org/10.1016/j.jhazmat.2016.03.067>
- [19] S. Mohan, J. Princz, B. Ormeci, M. C. DeRosa, *Nanomaterials* 9(9), 1258 (2019); <https://doi.org/10.3390/nano9091258>
- [20] T. H. Nguyen, Y. H. Kim, H. Y. Song, B. T. Lee, *Journal of Biomedical Materials Research B* 96(2), 225; <https://doi.org/10.1002/jbm.b.31756>
- [21] R. Nirmala, F. Sheikh, M. Kanjwal, J. Lee, S-J. Park, R. Navamathavan, H. Kim, *Journal of Nanoparticle Research* 13(5), 1917 (2011); <https://doi.org/10.1007/s11051-010-9944-z>
- [22] B. Pérez-Köhler, S. Benito-Martínez, F. García-Moreno, M. Rodríguez, G. Pascual, J. M. Bellón, J.M., *Surgery* 167(3), 598 (2020); <https://doi.org/10.1016/j.surg.2019.10.010>
- [23] J. Reinbold, T. Hierlemann, L. Urich, A. K. Uhde, I. Müller, T. Weindl, U. Vogel, C. Schlensak, H. P. Wendel, S. Krajewski, S., *Drug design, development and therapy* 11, 2753 (2017); <https://doi.org/10.2147/DDDT.S138510>
- [24] K. S. Siddiqi, A. Husen, R. a. Rao, R.A., 2018. *Journal of nanobiotechnology* 16(1), 14 (2018); <https://doi.org/10.1186/s12951-018-0334-5>
- [25] H.-P. Simmen, H. Battaglia, P. Giovanoli, J. Blaser, *Infection* 22(6), 386 (1994); <https://doi.org/10.1007/BF01715494>
- [26] P. Singh, K. Sen K. *Colloid and Polymer Science* 296(10), 1711 (2018); <https://doi.org/10.1007/s00396-018-4392-x>
- [27] G. A. Sotiriou, S. E. Pratsinis, *Current opinion in chemical engineering* 1(1), 3-(2011); <https://doi.org/10.1016/j.coche.2011.07.001>
- [28] B. Tang, J. Wang, S. Xu, T. Afrin, W. Xu, L. Sun, X. Wang, *Journal of Colloid and Interface Science* 356(2), 513 (2011); <https://doi.org/10.1016/j.jcis.2011.01.054>
- [29] R. Tankhiwale, S. K. Bajpai, *Journal of Colloid and Interface Science* 69(2), 164 (2009); <https://doi.org/10.1016/j.colsurfb.2008.11.004>
- [30] S. G. Taylor, P. J. O'Dwyer, *British Journal of Surgery* 86(4), 562 (1999). <https://doi.org/10.1046/j.1365-2168.1999.01072.x>
- [31] A. Trofimov, A. Ivanova, M. Zyuzin, A. Timin, *Pharmaceutics* 10(4), 167 (2018); <https://doi.org/10.3390/pharmaceutics10040167>
- [32] M. E. Vance, T. Kuiken, E. P. Vejerano, S. P. McGinnis, M. F. Hochella Jr, D. Rejeski, M. S. Hull, *Beilstein journal of nanotechnology* 6(1), 1769 (2015); <https://doi.org/10.3762/bjnano.6.181>
- [33] W. Wei, G. H. Ma, G. Hu et al., *Journal of American Chemical Society* 130, 15808 (2008); <https://doi.org/10.1021/ja8039585>